Engineering Applications of Artificial Intelligence 62 (2017) 286–301

Contents lists available at ScienceDirect

Engineering Applications of Artificial Intelligence

journal homepage: www.elsevier.com/locate/engappai

An evolutionary single Gabor kernel based filter approach to face recognition

Lingraj Dora [a], Sanjay Agrawal [b], Rutuparna Panda [b,*], Ajith Abraham [c]

[a] Department of Electrical and Electronics Engineering, VSSUT, Burla 768018, India
[b] Department of Electronics and Telecommunication Engineering, VSSUT, Burla 768018, India
[c] Machine Intelligence Research Labs (MIR Labs) Scientific Network for Innovation and Research Excellence, WA 98071-2259, USA

ARTICLE INFO

Article history:
Received 13 September 2016
Received in revised form
16 March 2017
Accepted 13 April 2017
Available online 27 April 2017

Keywords:
Face recognition
Gabor filter
Hybrid PSO-GSA
Eigenvalue

ABSTRACT

For the past few decades, Gabor filter banks have been used for extracting features in face recognition. The state-of-the-art approach for the design and selection of Gabor filter banks is based on a trial and error. This results in more computational complexity and higher response time. To overcome this problem, an attempt is made to design a single optimized Gabor filter instead of a filter bank for feature extraction. This approach improves the filter performance by significantly reducing the computational complexity and response time. The hybrid particle swarm optimization-gravitational search algorithm (PSO-GSA) is used for optimizing the parameters of the single Gabor filter. In this context, an evolutionary single Gabor kernel (ESGK) based filter approach is proposed for face recognition. The proposed method is used to extract Gabor energy feature vectors from face images. We also propose a new eigenvalue based classification approach for face recognition. This approach is derived from sparse based representation methods. The novelty in our paper is measurement of sparsity of the weighting coefficients of each training sample. The main contribution of the paper is two-fold. Firstly, investigation of ESGK approach, which is not found in the literature. Secondly, introducing a new eigen value based classifier. FERET, ORL, UMIST, GT and LFW databases are used to measure the efficiency of our proposed method. The results are compared with a holistic Gabor filter bank based recognition methods. It is witnessed that our proposed method outperforms the state-of-the-art methods.

1. Introduction

Face recognition (FR) is one of the effective ways of biometric identification. Over the past few decades, many researchers have contributed significantly to the development of FR techniques. FR is a technique for verifying the identity of a person based on statistical and geometrical features derived from a database of face images. Deriving features of the face images from a training database and comparing them with that of a test face image is carried out in recognition tasks. FR techniques have got a lot of applications in various areas such as person authentication, security access control, surveillance, criminal identification, etc. One of the important steps in FR technique is feature extraction from face images. Depending on the approach for extracting features, FR techniques are generally classified into two groups: (1) Feature-based methods and (2) Appearance-based methods. Feature-based methods extract physical or geometrical features from the face image such as eye distance, the shape of the eye, nose length etc., to identify a face image. Sometimes they also utilize facial expression, illumination or pose variation to discriminate face images (Barmpoutis et al., 2008; Blanz and Vetter, 2003; Brunelli and Poggio, 1993; Li et al., 2006). The appearance-based methods work on the whole face image for extracting features. Some of the popular appearance-based methods like Eigenfaces and Fisherfaces work well on different challenging conditions and occlusions like low light, facial hair and sunglasses (Chellappa et al., 1995; Matthew, 2001). Eigenfaces are based on principal component analysis (PCA) and Fisherfaces are based on linear discriminant analysis (LDA). In addition, PCA and LDA are popular methods used for dimension reduction. However, the linear methods like PCA and LDA are not capable enough for effective FR, as face images are interpreted as non-linear objects (Shah et al., 2013; Huang and Guan, 2015). Further, the limitation in such methods is that they require pre-processing steps both during training and testing of face images. Moreover,

* Corresponding author.
E-mail address: r_ppanda@yahoo.co.in (R. Panda).

http://dx.doi.org/10.1016/j.engappai.2017.04.011
0952-1976/

the methods perform well for classifying frontal images, but their performance degrades when classifying multi-view face images having rotation and tilt.

To overcome the above mentioned limitations, Gabor filter bank is a suitable approach for extracting features from face images in an effective manner. Gabor filters are particularly efficient due to its biological relevance and best computational properties. Further, they have the ability to acquire significant visual properties like spatial localization, frequency and orientation selectivity. These make them attractive to be used in the field of face recognition (Abate et al., 2007; Cament et al., 2015; Daugman, 1988, 1985; Raghavendra et al., 2016; Shen and Bai, 2006; Zhao et al., 2012). Classically, Gabor-based methods for FR uses a bank of filters having five scales and eight orientations (Lades, 1993; Wiskott, 1997). In Liu and Wechsler (2003) a bank of 40 Gabor filters having five scales and eight orientations are used for extracting facial features. Then PCA followed by independent component analysis and probabilistic reasoning model is used for FR. In Li et al. (2012) Gabor filter-based method used a regressor in conjunction with a coupled bias-variance for the FR. In local matching Gabor (LMG) method, a total of 4172 Gabor jets are used, which significantly increases the computational time (Perez et al., 2011a, 2011b; Zou et al., 2007).

Serrano et al. (2011) used the 6-way analysis of variance method (ANOVA) to find an optimal Gabor filter bank. The optimal bank contains Gabor filters having six frequencies and narrower Gaussian widths. The parameters of the optimal Gabor filter bank are robust enough to recognize faces under different challenging conditions like pose variation, occlusion, facial expression and illumination variation. In Cament et al. (2015) Gabor filter is efficiently used for FR under pose variation. In this approach active shape model is used to shift Gabor filter, depending on face pose. Also, the local statistical model is used to consider local changes in face images due to pose variation (Vu and Caplier, 2009). FR under pose variation still remain a challenging task due to misalignment, obscure facial features, lack of knowledge about subspace of pose variant face images, etc. In addition, arbitrary rotation of face images also increases discrimination in faces of same person which leads to incorrect recognition. Many researchers have proposed 2D and 3D methods for FR, taking pose variation into consideration. 3D morphological model for FR used an input face image to build a 3D model (Blanz and Vetter, 2003; Paysan et al., 2009).

Recently, Gabor filter-based approaches are also extensively used in other image processing areas like texture segmentation, text detection, medical image processing, etc. (Aradhya and Pavithra, 2014; Cruz-Aceves et al., 2016; Li et al., 2013; Raghavendra et al., 2016). The Gabor filter bank has been used as a tool for classification of breast cancer as normal, benign or malignant (Raghavendra et al., 2016). ANOVA method is used to obtain optimal Gabor filter parameters. It is effectively used to extract texture features from mammogram images. Then locality sensitive discriminant analysis is used to reduce the dimension of extracted features. The reduced features are then classified using classification method. Recently, artificial intelligence (AI) techniques are effectively used to obtain an optimal Gabor filter bank. Sun et al. (2005) proposed an evolutionary Gabor filter optimization technique to obtain the optimal set of filter bank. The authors applied Genetic Algorithm (GA) followed by an incremental clustering method for optimizing and selecting filters. In their approach, GA was used to select optimized filters (from a bank of filters). The authors selected nineteen optimized filters from a bank of twenty-four filters (for a threshold factor of 3). The method has been used for vehicle detection only.

However, all the above methods involve selection of appropriate number of filters (filter bank) consisting of more than 40 filters, to extract sufficient features. Therefore, as the number of filters in the bank increases, the computational cost in the method also increases, because Gabor filter bank results in a huge set of features. In addition, they also suffer from a large response time. To overcome the above problems, we propose an AI-based single Gabor filter as shown in Fig. 1. AI technique is used to obtain a single optimized filter which reduces the dimension of feature space as well as the computational cost and the response time.

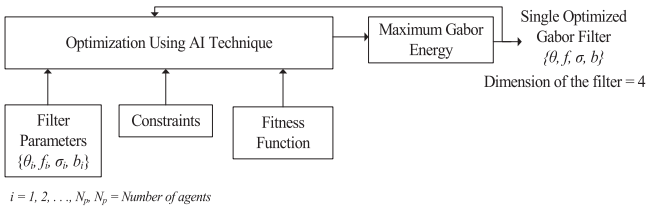

Fig. 1. Block diagram of AI-based Gabor filter.

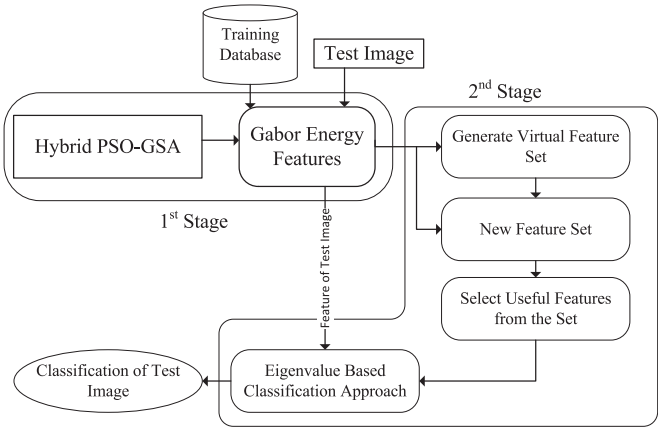

Fig. 2. Block diagram of the proposed method.

In this paper, we propose an ESGK approach to face recognition, shown in Fig. 2.

The proposed method consists of two stages. Firstly, hybrid PSO-GSA is used to obtain a single optimized Gabor filter by selecting optimal filter parameters. The optimized Gabor filter is used to extract features from the face images. Secondly, the extracted features are used to generate a virtual feature set. A new feature set is formed by combining original and virtual feature set. A new eigenvalue based classification approach is proposed to identify the unknown test face images by considering only useful features of the new set. The proposed method uses a single optimal Gabor filter instead of a bank of filters. This results in significant reduction of the computational complexity and response time. Furthermore, the proposed method works well for frontal face images as well as for face images with pose variation.

The rest of the paper is organized as follows: Section 2 presents a brief explanation about Gabor filter bank approach. Section 2.2 explains our proposed method. Experimental results and discussions are presented in Section 3. Finally, Section 4 is the conclusion.

2. Gabor filter bank approach

2.1. Gabor filter method

The Gabor filter exhibits a strong characteristic of orientation selectivity and spatial locality and are optimally localized in space and frequency domain. The Gabor filters are defined as (Daugman, 1988, 1985; Kruizinga a nd Petkov, 1999; Liu and Wechsler, 2003; Raghavendra et al., 2016):

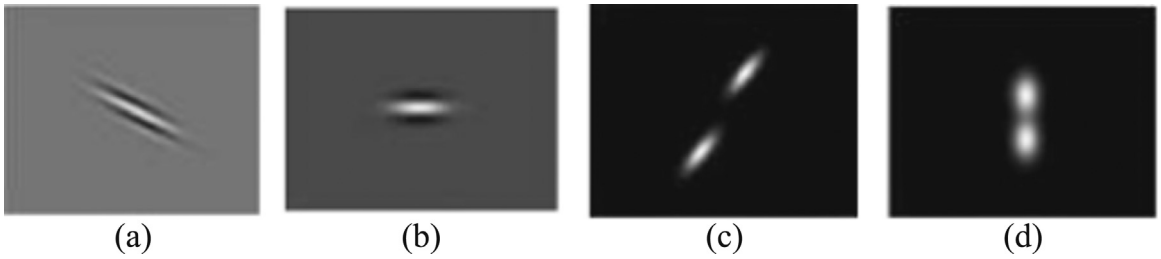

Fig. 3. Gabor filters in spatial domain and frequency domain. (a) spatial response for parameter set P={30°, 0.2, 0.5, 1}. (b) spatial response for parameter set P={0°, 0.1, 0.5, 1}. (c) frequency response for filter in (a). (d) frequency response for filter in (b).

$$g(x,y) = exp\left(-\frac{\tilde{x}^2+\sigma^2\tilde{y}^2}{2\mu^2}\right)\cos\left(2\pi f\tilde{x}+\varnothing\right)$$
$$\tilde{x} = (x-x_o)cos\theta - \left(y-y_o\right)sin\theta$$
$$\tilde{y} = (x-x_o)\sin\theta + \left(y-y_o\right)\cos\theta \quad (1)$$

Where the symbols carry usual meaning as defined in Daugman (1988). The ratio μ/λ gives the spatial bandwidth b of the filter and the relationship between them is given as:

$$\frac{\mu}{\lambda} = \frac{1}{\pi}\sqrt{ln2/2} * \frac{2^b+1}{2^b-1} \quad (2)$$

In our filter design, we have used $\phi = \pi$ for symmetric filter and $\phi=\pi/2$ for anti-symmetric filter. The Gabor filter as given in Eq. (1) can be designed by choosing proper values of the four parameters in $P=\{\theta, f, \sigma, b\}$. Fig. 3(a) and (b) show Gabor filters for two different parameters in spatial domain. Fig. 3(c) and (d) show the same filter responses in frequency domain obtained by taking their Fourier transform. Thus, different parameters give different filter responses, causing difficulty in designing filters for pattern classification task like FR. This problem can be avoided by optimally selecting the parameters θ, f, σ, b in P.

For example, if a task requires N number of filters, then we have to optimize $4N$ parameters while considering the filter bank approach. However, in our approach, we need to optimize only 4 parameters. Thus, the dimension is reduced from $4N$ to 4, which represents a single filter, resulting in reduction of the computational complexity and time.

2.2. Gabor energy feature representation

The Gabor filter response to a face image is the convolution of Gabor filter as given by Eq. (1) with the face image. For a face image $I(x, y)$, the response of Gabor filter is given as:

$$R(x,y) = I(x,y) \otimes g(x,y) \quad (3)$$

where $\otimes$ represent the convolution operator. For a particular parameter set $P=\{\theta, f, \sigma, b\}$ the response R contains features of the face image in that local scale and orientation. However, filters with different parameter set results in different responses for the same face image. A bank of filters having different parameters will be able to capture features of the face image in all possible scales and orientations and can be used to derive local and discriminatory features, as shown in Fig. 4.

The response of a symmetric Gabor filter bank having five (05) scales and eight (08) orientations as shown in Fig. 5(b) to an example face image in Fig. 5(a) is shown in Fig. 5(c). Similarly, Fig. 6 (c) shows the response of anti-symmetric Gabor filter having same scales and orientations. The response R contains both the real and the imaginary parts of the Gabor transform.

In this scheme, a face image is passed through a set of filters having different scales, orientations and phases. The features

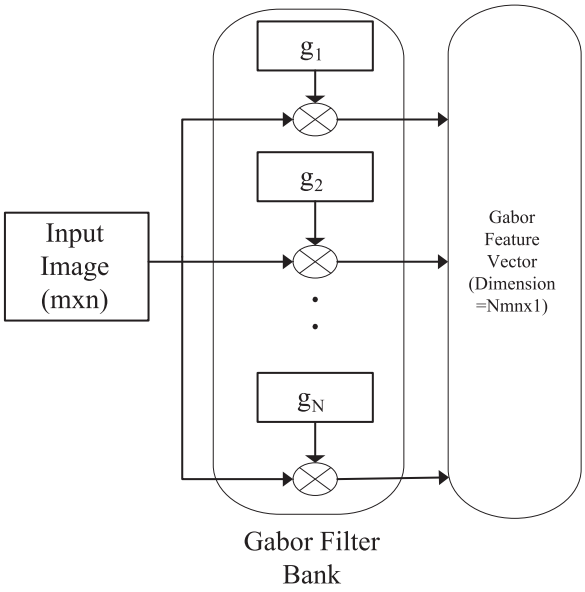

Fig. 4. Feature extraction of a face image using Gabor filter bank.

obtained by combining the response of the filter to the phase pairs is called Gabor energy feature. For a filter bank consisting of N number of filters, the Gabor energy is given as:

$$E(x,y) = \sqrt{R^2_{\theta,f,\sigma,b,\pi}(x,y)+R^2_{\theta,f,\sigma,b,\pi/2}(x,y)} \quad (4)$$

where, $R^2_{\theta,f,\sigma,b,\pi}$ and $R^2_{\theta,f,\sigma,b,\pi/2}$ are the response of the symmetric and anti-symmetric Gabor filters respectively, having phase pairs π and $\pi/2$. Fig. 7 shows Gabor energy feature representation of the example face image (Figs. 5(a) and 6(a)) by combining the responses of symmetric and anti-symmetric filter bank given in Figs. 5(c) and 6(c). While designing the filter bank, different values of scale and orientation are chosen in such a way that it approximately covers the entire spatial-frequency domain. If the filter bank is designed by taking a large number of scales and orientations, computational complexity and filter response time increases. On the other hand, if it is designed with a small number of scales and orientations, its response will be degraded for the face images, which may contain discriminating features in some other scales and orientations.

Thus, the feature discrimination performance of filter bank solely depends on the optimal choice of scale and orientation parameters. In this paper, we propose an ESGK approach which has dual advantage. It eliminates the problem of computational complexity and large response time associated with filter bank design having large number of parameters. Additionally, it also eliminates the problem of degradation of discriminating features in case of filter design with a smaller number of parameters. In this

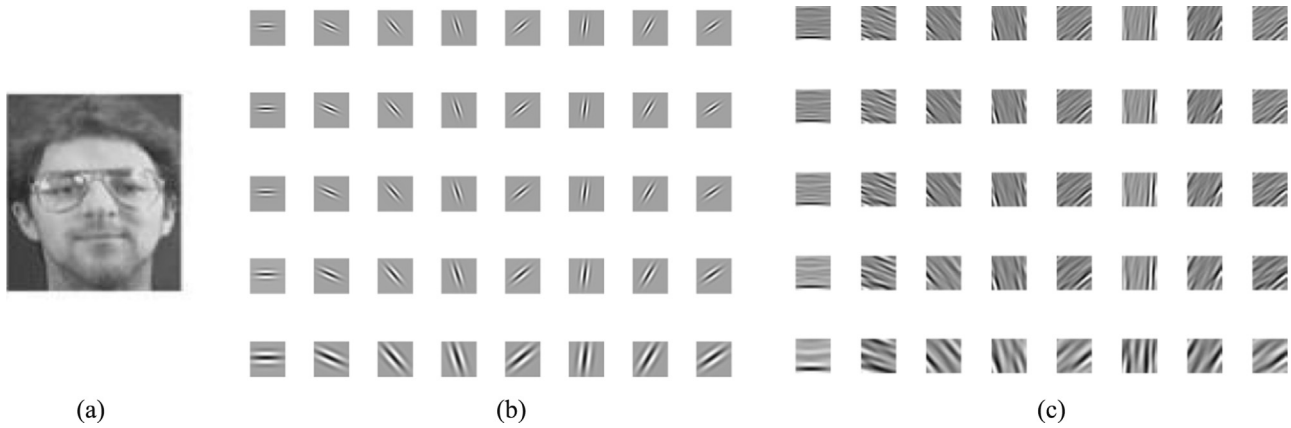

Fig. 5. Response of a symmetric Gabor filter bank. (a) Example face image. (b) symmetric Gabor filter bank having five scales and eight orientations. (c) Response of symmetric Gabor filter bank to face image in (a).

paper, we have designed a single filter that contains the optimal orientation and spatial frequency. A global optimum filter parameter set is obtained by using hybrid PSO-GSA technique, corresponding to maximum Gabor energy. The response of this filter to a face image also contains the relevant global discriminatory features. As a single filter is used to extract the features from the face images instead of bank of filters, it significantly reduces the complexity and feature extraction time.

3. Hybrid PSO-GSA

3.1. Particle swarm optimization

PSO is a population-based stochastic optimization tool/algorithm originally proposed by Kennedy and Eberhart (1995). The particle's velocity and position are updated as:

$$v(t+1) = w(t) \times v(t) + c_1 \times r_1 \times \left(pbest(t) - x(t)\right) + c_2 \times r_2 \times \left(gbest(t) - x(t)\right) \quad (5)$$

$$x(t+1) = x(t) + v(t+1) \quad (6)$$

$$w(t) = rand \times \frac{t}{t_{max}} \times (w_{max} - w_{min}) + w_{min} \quad (7)$$

where, $x(t)$ and $v(t)$ are position and velocity of particle at iteration t. c_1 and c_2 are two positive acceleration coefficients used to control the effect of p_{best} and g_{best} in the search domain. r_1 and r_2 are two random numbers in [0,1]. $w(t)$ is the inertia weight in the range w_{max} and w_{min} and it controls the influence of previous velocities on new velocities. t_{max} is the maximum number of iterations.

3.2. Gravitational search algorithm

GSA is also a population based optimization algorithm originally proposed by Rashedi et al. (2009). It is based on Newton's law of gravitation and mass interaction. The detailed GSA steps are given as follows:

Step 1. Agents (masses) initialization: At first positions of N_a number of agents (masses) is randomly initialized within the search domain as:

$$X_i = \left\{ x_i^1, \ldots, x_i^d, \ldots, x_i^D \right\}, i=1, 2, \ldots, N_a \quad (8)$$

where, x_i^d is the position of ith agent having dimension d which is consider as a solution, D is the dimension of search domain and N_a is the total number of agents in the population.

Step 2. Fitness function evaluation for each agent: In each iteration fitness of all agents are evaluated along with *best* and

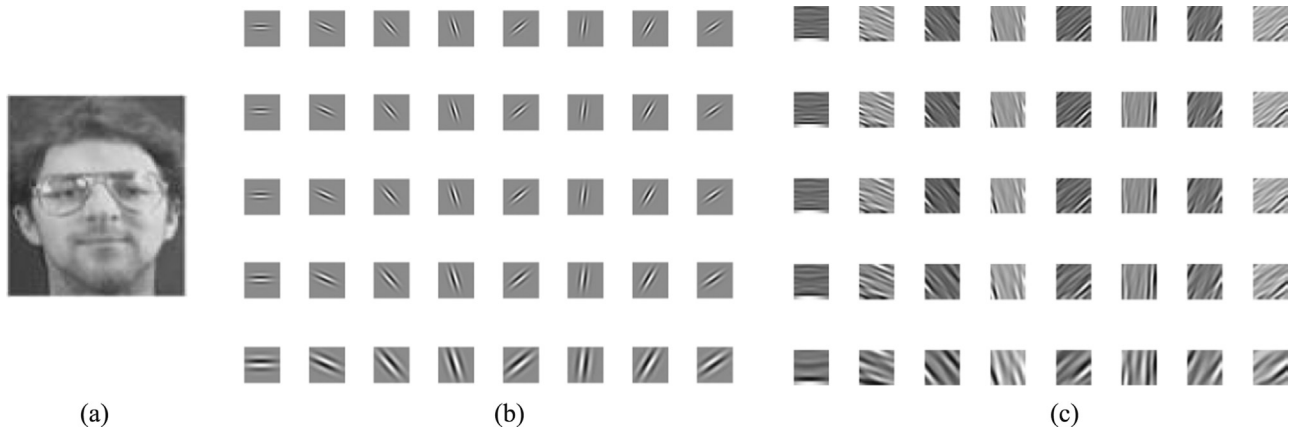

Fig. 6. Response of an anti-symmetric Gabor filter bank. (a) Example face image. (b) Anti-symmetric Gabor filter bank having five scales and eight orientations. (c) Response of anti-symmetric Gabor filter bank to face image in (a).

Fig. 7. Gabor energy feature representation of an example face image.

Step 1: Let X be a training dataset of M face images. Each image is of size $'w \times h'$.
Initialization:
Step 2: A swarm of S particles is created, each having a dimension 4. Each particle's position is initialized with four parameters $P = \{\theta, f, \sigma, b\}$.
Optimization:
Step 3: Hybrid PSO-GSA is used to update S such that the fitness function given by Eq. (21) is minimized.
Step 4: Hybrid PSO-GSA generates an optimal filter for which fitness function is minimized.
Step 5: The optimal Gabor filter is used to extract the facial feature from M training face images and from test face image.
Step 6: The optimal feature vectors are used to generate virtual feature vector using Eq. (22).
Step 7: K most useful feature vectors are selected from new feature vector using Eq. (23).
Classification:
Step 8: Average feature vector and the covariance matrix of the K selected feature vectors are calculated using Eq. (25) and (26), respectively.
Step 9: Eigenvectors representation of the training images is calculated Eq. (27).
Step 10: Coefficient w is obtained from Eq. (28).
Step 11: Then Eq. (29) and (30) are used to calculate the residual distance D_r for the test sample.
Step 12: The test sample y is then classified into the class that has the minimum distance.

Fig. 8. Pseudocode of the proposed method.

worst fitness values all agents as:

$$best(t) = \min_{j\in\{1\cdots N_a\}} fitness_j(t) \tag{9}$$

$$worst(t) = \max_{j\in\{1\cdots N_a\}} fitness_j(t) \tag{10}$$

where, $fitness_j(t)$ is the fitness value of jth agent at iteration t.

Step 3. Computation of gravitational constant $G(t)$: In each iteration gravitational constant $G(t)$ is computed as:

$$G(t) = G_0 \exp\left(-\alpha \frac{t}{t_{max}}\right) \tag{11}$$

According to Rashedi et al. (2009), G_0=100 and $\alpha = 20$.

Step 4. Mass of agents: Then in each iteration mass of agents are calculated as:

$$q_i(t) = \frac{fitness_i(t) - worst(t)}{best(t) - worst(t)} \tag{12}$$

$$M_i(t) = \frac{q_i(t)}{\sum_{j=1}^{N_a} q_j(t)} \tag{13}$$

where, $M_i(t)$ is the mass of ith agent at iteration t.

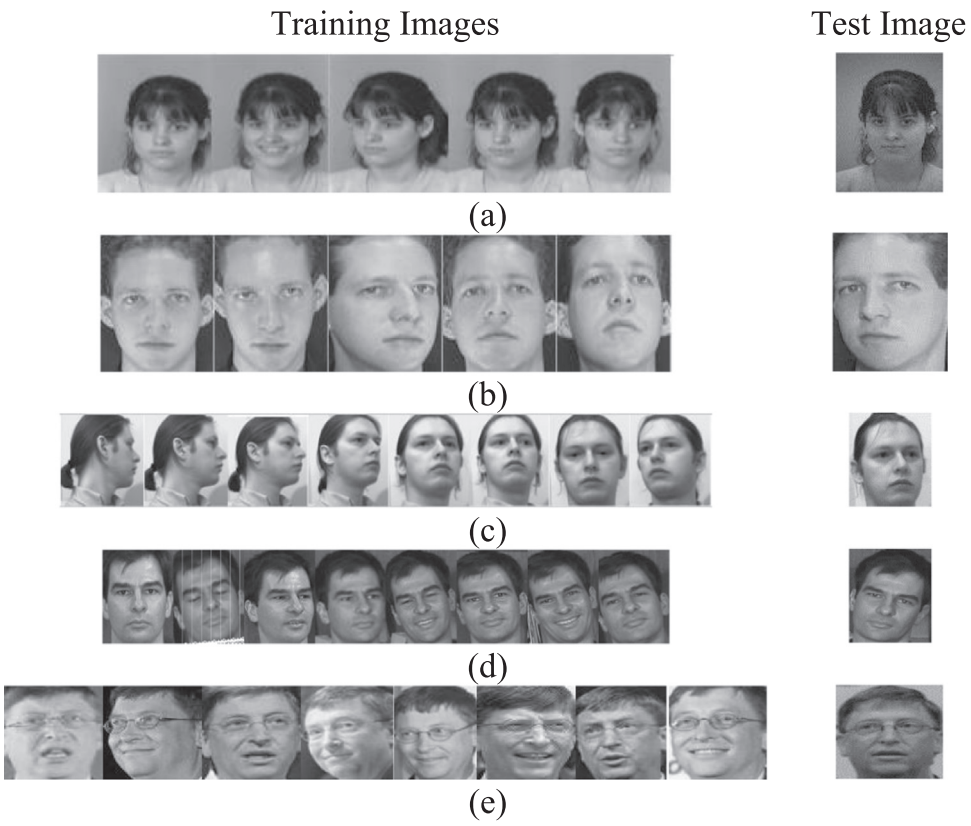

Fig. 9. Examples of training and test face images. (a) FERET database. (b) ORL database. (c) UMIST database. (d) GT database. (e) LFW database.

Step 5. Acceleration of agents: In each iteration acceleration of agents is calculated as:

$$a_i^d(t) = \sum_{j \in kbest, j \neq i} rand_j \, G(t) \frac{M_j(t)}{R_{ij}(t) + \varepsilon} \left(x_j^d - x_i^d \right), \; d = 1, 2 \cdots D \; , j = 1, 2 \cdots N_a \tag{14}$$

$$R_{ij}(t) = \left\| X_i(t), X_j(t) \right\| \tag{15}$$

where, $a_i^d(t)$ is the acceleration of *ith* agent having dimension *d*, *randj* is a random value in the range [0,1], ε is a constant, $R_{ij}(t)$ is the Euclidean distance between agents *i* and *j* respectively, k_{best} is the set of agents having *best* fitness value and biggest mass. It is a function of time having initial value K_0 and gradually decreases to 1.

Step 6. Updating velocity and position of the agents: On each iteration, velocity and position of agents are updated as:

$$v(t+1) = rand \times v(t) + a_i^d(t) \tag{16}$$

$$x(t+1) = x(t) + v(t+1) \tag{17}$$

where, $x(t)$ and $v(t)$ are position and velocity of an agent at iteration *t*.

Step 7. Step 2 – 6 is repeated until maximum iteration is not reached or stopping criterion is met.

Table 1
Comparison of fitness function values.

Optimization technique	Best fitness function value
GA	0.0010
PSO	9.8848e−04
GSA	9.6292e−04
Hybrid PSO-GSA	**9.5393e−04**

3.3. PSO-GSA algorithm

The hybrid PSO-GSA is proposed which possess the abilities of both PSO and GSA approaches (Jiang et al., 2014). In PSO-GSA both the algorithms work in a serial manner. In this algorithm, a particle position is updated based on the velocity as given in Eq. (5) and acceleration given in Eq. (16). Thus the velocity update in hybrid PSO-GSA is given as:

$$v(t+1)_{PSO-GSA} = c_3 \times r_3 \times v(t+1)_{PSO} + c_4 \times (1 - r_3) \times v(t+1)_{GSA} \tag{18}$$

where, $v(t+1)_{PSO}$ and $v(t+1)_{GSA}$ are velocity and acceleration updating formula from PSO and GSA respectively. c_3 and c_4 are acceleration coefficients which handle the velocity and acceleration. r_3 is a random number generated in the interval [0,1]. In every iteration position of a particle is updated as:

$$x(t+1)_{PSO-GSA} = x(t)_{PSO-GSA} + v(t+1)_{PSO-GSA} \tag{19}$$

4. Proposed ESGK approach

In this paper, ESGK approach is used for FR by implementing an optimized Gabor filter to obtain features from face images.

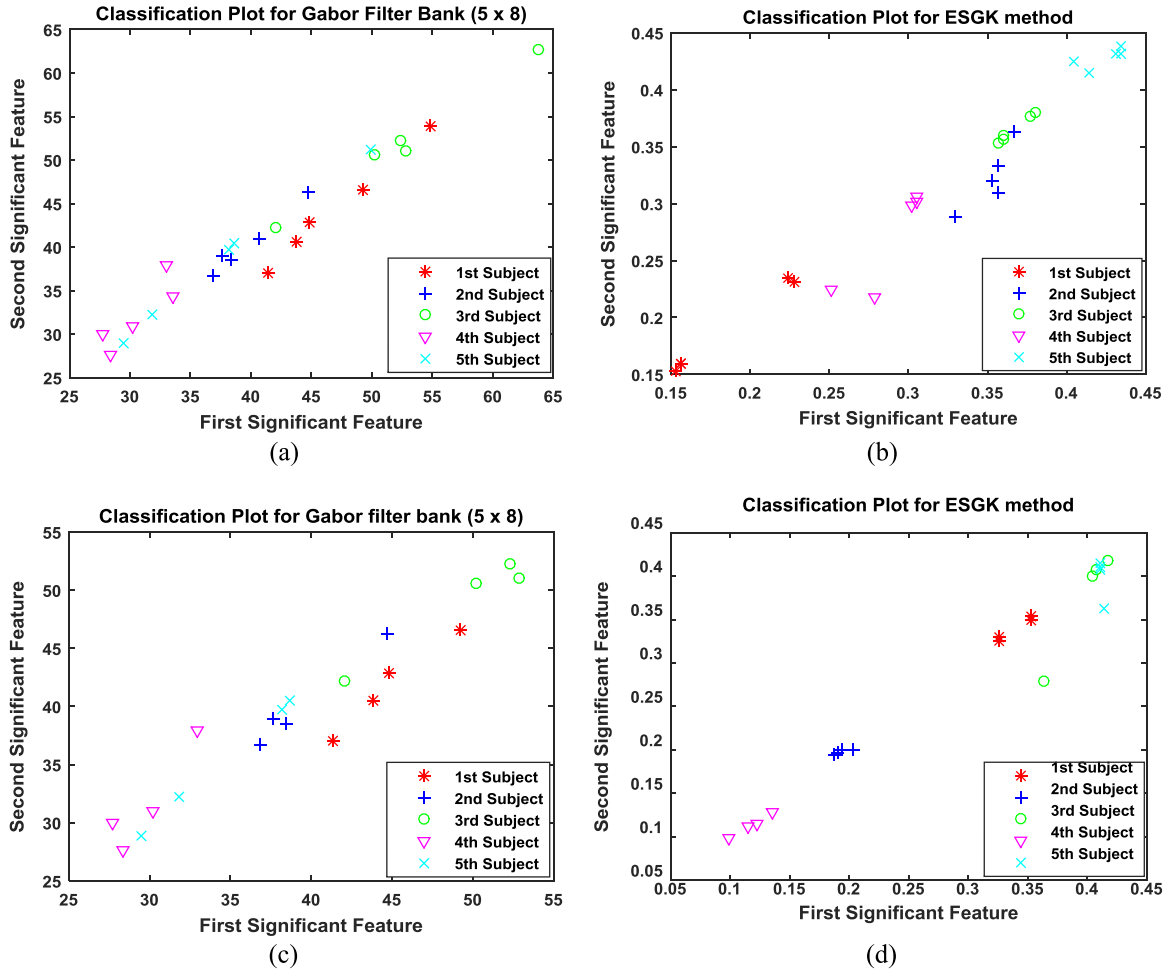

Fig. 10. 2D Classification plots using two most significant features of training face images of FERET database. (a) 25 training images of 5 different subjects obtained using Gabor filter bank (40 filters) method. (b) 25 training images of 5 different subjects obtained using ESGK method. (c) 20 training images of 5 different subjects obtained using Gabor filter bank (40 filters) method. (d) 20 training images of 5 different subjects obtained using ESGK method.

These features are then used to synthesize a virtual set of feature vectors. A modified feature vector set is formed by combining the original feature vectors and the virtual feature vectors. A new eigenvalue-based classification approach is also proposed, which exploits the virtual feature vectors along with the features of test face image, to perform the recognition. Recently, hybrid optimization techniques are gaining more attention for solving problems. The hybrid techniques use the complementary strength of individual optimization methods. This has motivated us to apply a hybrid technique for optimizing Gabor filters. Hybrid PSO-GSA is used here to optimize the parameter set of Gabor filter. To design a filter, hybrid PSO-GSA uses a particle x having dimension P as discussed in Section 2.1. The position of each particle x is updated using Eq. (19), and the velocity is updated using Eq. (18). The proposed objective function is optimized using PSO-GSA. The global best position of the particle represents the single optimal Gabor filter. The optimal Gabor filter is then used to obtain Gabor energy feature vectors from face images.

4.1. Gabor filter parameter selection

The hybrid PSO-GSA algorithm initially generates a random set of Gabor filter parameters constrained to be defined within a range. The range of the orientation parameter θ is given as: $\theta \in [0, \pi)$. The parameter f, which is the spatial frequency of Gabor filter, is application dependent. In this work, we have used the value of f within the range $[0,0.5]$. The shapes of the elliptic Gaussians should be similar for the 2D Gabor filter model. The aspect ratio σ is a dimensionless quantity in the range [0,1]. It is computed by considering the ratio of the minor axis to the major axis. There is no categorically desired value of the aspect ratio. However, it is observed experimentally that the values in the range 0.23–0.92 gives a reasonable shape from (nearly 5 to 1 elongation) to nearly round (Jones and Palmer, 1987).

In this paper, the spatial aspect ratio, is limited to $[0.23,0.92]$. From the study, it is observed that the range of the spatial bandwidth b for most of the receptive cells is within 1.0 – 1.8 octaves (Kruizinga and Petkov, 1999). The above constraints are used to generate the four parameters of a Gabor filter.

4.2. The fitness function for ESGK method

The fitness function used in hybrid PSO-GSA algorithm for selecting optimal filter is the Gabor energy vector. The fitness function is given as:

$$F = \sum \sum E(x, y) \tag{20}$$

$$F_{opt} = min\{-F\} \tag{21}$$

The optimization algorithm searches for the filter for which the Gabor energy E is maximized. In Eq. (21), the negative of the

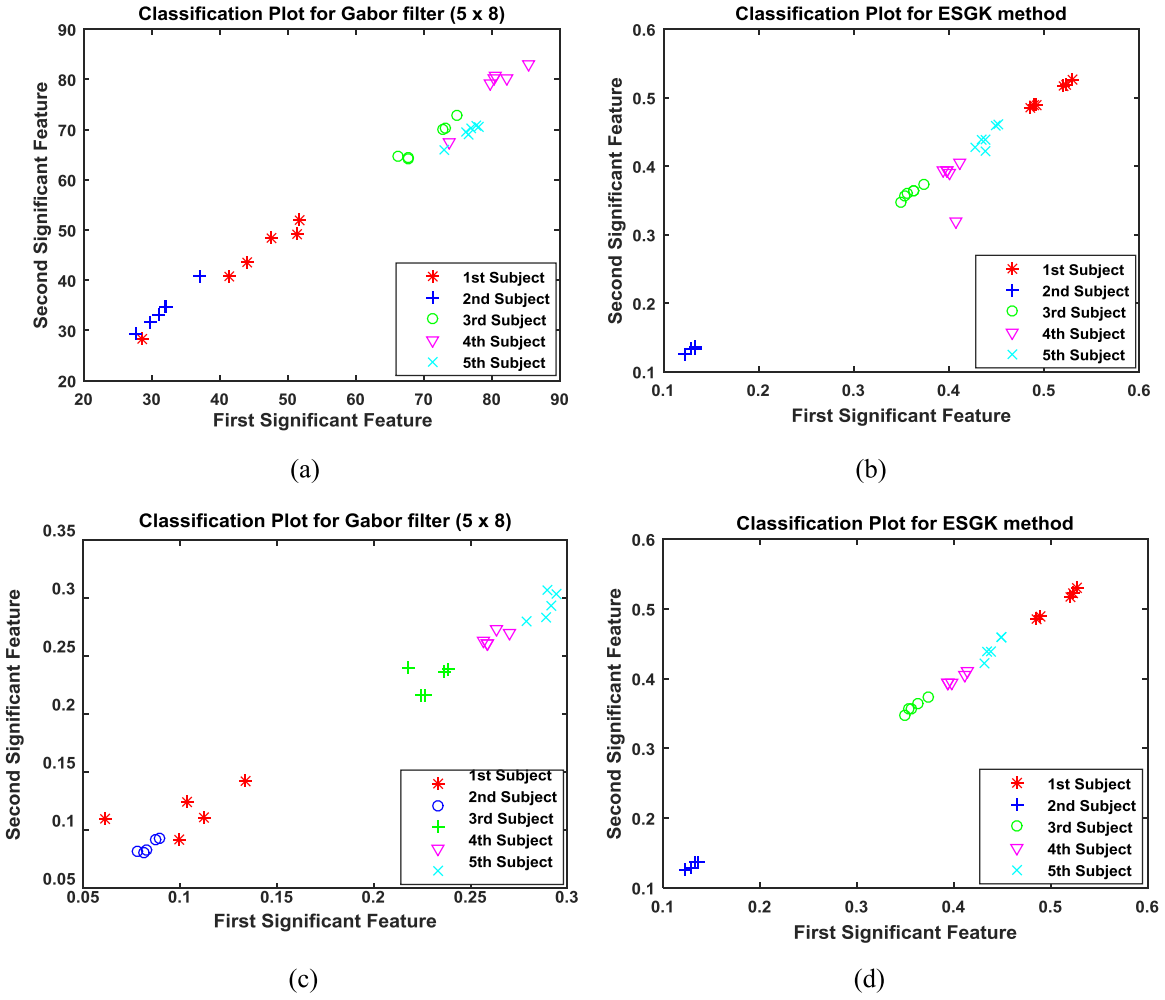

Fig. 11. 2D Classification plots using two most significant features of training face images of ORL database. (a) 30 training images of 5 different subjects obtained using Gabor filter bank (40 filters) method. (b) 30 training images of 5 different subjects obtained using ESGK method. (c) 25 training images of 5 different subjects obtained using Gabor filter bank (40 filters) method. (d) 25 training images of 5 different subjects obtained using ESGK method.

objective function is minimized, which is a usual practice with the optimization community (Manikandan et al., 2014).

4.3. Generation and selection of useful feature vectors

After extracting the Gabor energy feature vectors from both the training and the test face images, virtual feature vector set is generated from the extracted feature vectors of the training images. These virtual feature vector set is combined with the original Gabor energy feature vector set to form a new feature vector set. The virtually generated feature vectors reduce the uncertainty of the feature space. As the training database contains limited number of face images of a particular subject, they provide inadequate information about a face image such as pose variation, facial expression, occlusion etc.

Let $E=[E_1, E_2,\ldots,E_L]$ be the number of Gabor energy feature vectors extracted from the training images. Where, L is the total number of training images having C number of classes. Then a virtual feature vector is generated by taking every two feature vectors from ith class as given below (Xu et al., 2014):

$$E_j^v = \frac{\left(E_i^t + E_i^s\right)}{2} \text{ for } j=1, 2, \ldots, C_v \tag{22}$$

where, E_i^t and E_i^s are two feature vectors from ith class, E_j^v is the generated virtual feature vector and C_v is the number of virtual feature vectors generated in ith class. The generated virtual feature vectors are more capable of representing possible variations in the features of face images. After the generation of virtual feature vectors from all the C classes, a new feature vector set is formed by combining original feature vectors and virtual feature vectors. The new feature set contains different possible representation and the ability to classify the features of test image. However, new feature set also contains some unusual feature vectors which could result in misclassification of test sample. Hence, Euclidean distance measure is used to select only K useful feature vectors from the new feature vector set having minimum distance from test feature vector by using

$$d_j = \left\| y - E_j \right\|_2 \tag{23}$$

where a small d_j means that the feature vector E_j is more similar to the test image feature vector y.

4.4. Eigenvalue-based classification approach

In this section, an eigenvalue-based classification approach is used for classification of test images. The selected K most useful Gabor energy feature vectors obtained from Eq. (23) are used for the purpose. The eigenvalue-based classification approach assumes feature of the test image as a linear combination of features of K selected training images, given as:

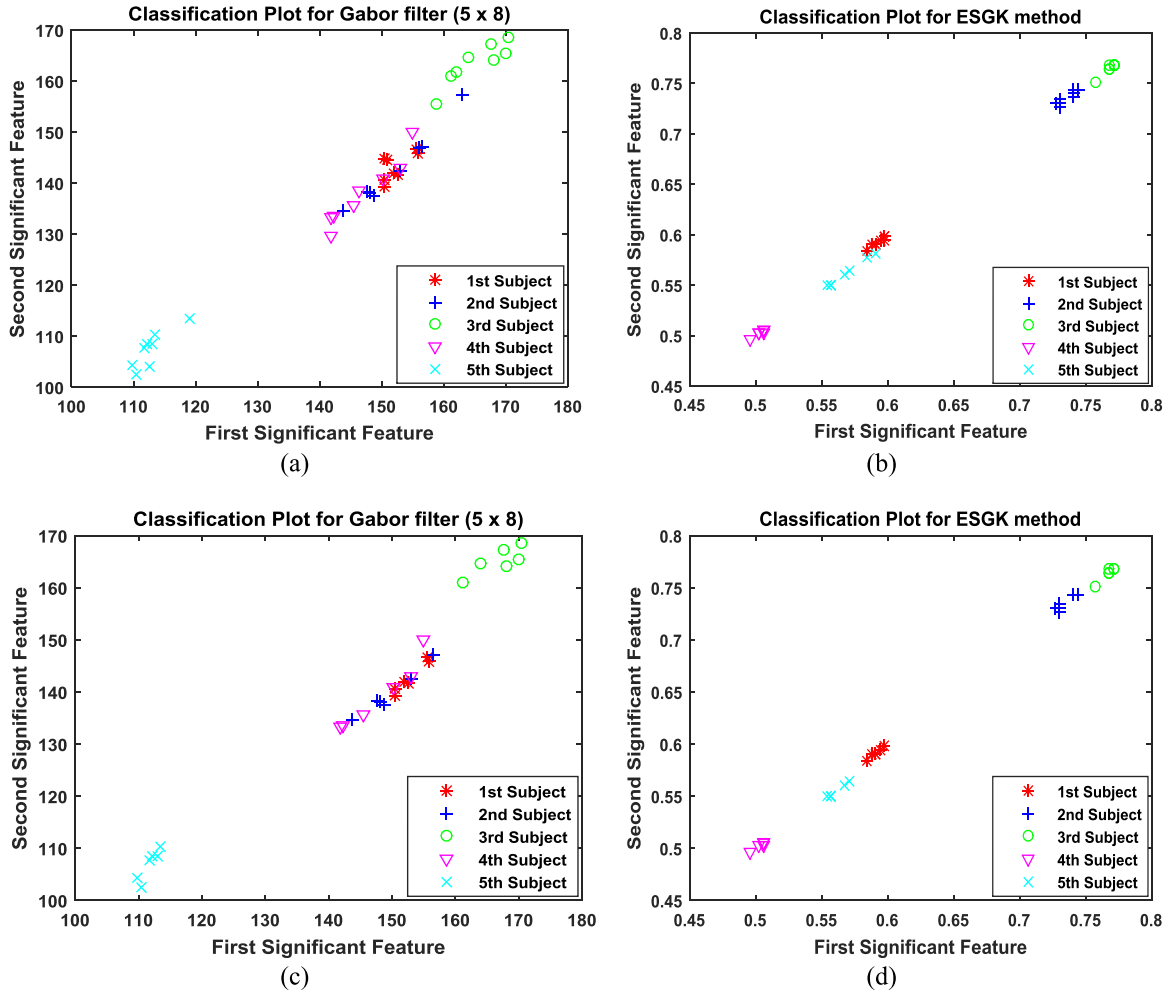

Fig. 12. 2D Classification plots using two most significant features of training face images of UMIST database. (a) 40 training images of 5 different subjects obtained using Gabor filter bank (40 filters) method. (b) 40 training images of 5 different subjects obtained using ESGK method. (c) 30 training images of 5 different subjects obtained using Gabor filter bank (40 filters) method. (d) 30 training images of 5 different subjects obtained using ESGK method.

$$y = w_1\tilde{E}_1 + w_2\tilde{E}_2 + \cdots + w_K\tilde{E}_K \tag{24}$$

w_i are the coefficients and $\tilde{E}_i$ are the K selected useful feature vectors for $i = 1,2, \ldots, K$. We have used eigenvalue decomposition approach to solve and obtain the solution for w. In this step, first we calculate the vectors which best describes the distribution of features within the domain. These vectors are the eigen-vectors having non-zero eigenvalues of the covariance matrix corresponding to the original K selected feature vectors. The average of the K selected useful feature vectors is calculated as:

$$\psi = \frac{1}{K}\sum_{i=1}^{K}\tilde{E}_i \tag{25}$$

Let $\Gamma_i = \tilde{E}_i - \psi$ represents the difference of each selected feature vector from the average feature vector. Then the covariance of the selected feature vectors is defined as:

$$\Omega = \frac{1}{K}\sum_{i=1}^{K}\Gamma_i\Gamma_i' \tag{26}$$

Let Δ represents the eigen-vectors of covariance matrix Ω corresponding to non-zero eigenvalues. The optimal linear least square representation of the K selected feature vectors are obtained as:

$$\xi = \Gamma'\Delta \tag{27}$$

where $\xi = [\xi_1, \xi_2, \ldots, \xi_m]$ are the eigen-vectors representation of the selected feature vectors preserving variance. These eigenvectors are used to project the feature vectors of both training and test images into a subspace using linear transformation $Z = \xi'\Gamma'$ and $\tilde{y} = \xi^i y'$, respectively. The solution for the coefficient w is obtained as:

$$w = Z'\tilde{y} \tag{28}$$

Since the K feature vectors might belong to different classes, the sum of the contribution of all K feature vectors is computed to represent the test feature vector. Then the sum is exploited to classify the test sample. For example, if all the feature vectors from the rth class are $E_1, E_2, \ldots, E_{C_t}$, then the sum of the samples to represent the test sample of the rth class will be:

$$S_r = \sum_{i=1}^{C_t} w_i E_i \tag{29}$$

where $w_1, \ldots, w_{C_t}$ are the coefficients of $E_1, E_2, \cdots, E_{C_t}$, respectively. C_t is the number of feature vectors selected from the rth class. The distance of the test feature vector from S_r is calculated as:

$$D_r = \|y - S_r\|_2 \tag{30}$$

Smaller is the distance D_r, the greater is the contribution to the test sample. The test image y belongs to a class that has the smallest distance. The pseudocode of the proposed method is shown in Fig. 8.

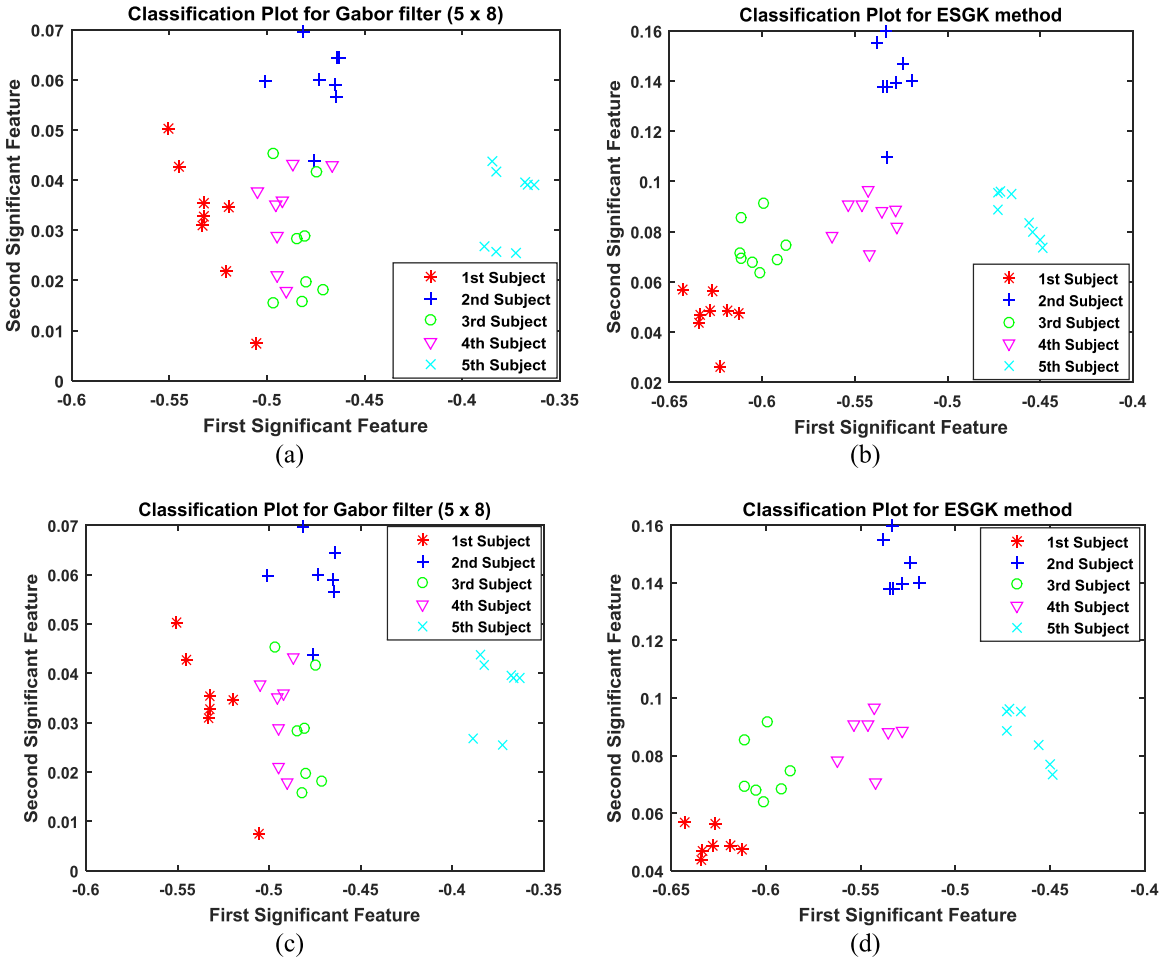

Fig. 13. 2D Classification plots using two most significant features of training face images of GT database. (a) 40 training images of 5 different subjects obtained using Gabor filter bank (40 filters) method. (b) 40 training images of 5 different subjects obtained using ESGK method. (c) 35 training images of 5 different subjects obtained using Gabor filter bank (40 filters) method. (d) 35 training images of 5 different subjects obtained using ESGK method.

5. Results and discussions

Five face image databases, FERET (Phillips, 2004; Phillips et al., 2000), ORL (http://www.com-orl.co.uk/facedatabase.html), UMIST (http://images.ee.umist.ac.uk/ danny/database.html), GEORGIA TECH (GT) (http://www.anefian.com/face reco.htm) and LFW (Wang et al., 2012) are used to demonstrate the performance of our proposed method. All the experiments are carried out on a MAC OSX environment using Intel core i5. All the programs are executed in MATLAB. From FERET database, we have used a sub-category of images with their names containing two-character string: *ba*, *bj*, *bk*, *bd*, *be*, *bf* and *bg*. This two lowercase character string indicates the kind of imagery. The string *ba* represents frontal "b" series, *bj* indicates alternative expression to *ba* and *bk* represents different illumination to *ba*. The string *bd*, *be* represents the subject facing to his left and *bf*, *bg* indicates the subject facing to his right. The images in this subset have illumination and expression variation, pose variations of $\pm 15^0$,$\pm 25^0$. This subset contains 1400 face images of 200 subjects, each subject having seven images. For evaluation of our proposed method, we have conducted two experiments on this subset. In the first experiment, we have randomly selected five images of each subject for training and the remaining two images for testing. In the second experiment, we have used randomly selected four images of each subject for training and the remaining three images for testing. All the images in the two experiments are cropped and resized to 40×40 pixels. The ORL database consists of 400 face images of 40 different subjects having 10 face images each. In this database, images of some subjects are taken at different times having varying lighting condition, facial expressions and face details (glasses/ no glasses). For ORL database, at first all the face images are cropped and resized to 32×32 pixels to conduct two different experiments. In the first experiment, we have selected first six images of each subject for training and rest four images for testing. In the second experiment, first five images of each subject are used for training and the remaining five images are used for testing.

The UMIST database contains 1012 face images of 20 different subjects. Here, all the face images are cropped and resized to 32×32 pixels. For UMIST database, we have conducted two experiments. In the first experiment, we have randomly selected eight images of each subject for training and the remaining images are used for testing. In the second experiment, we used randomly six images of each subject for training and the remaining images for testing. The GT database contains 750 images of 50 different subjects having 15 images for each subject. In this database, images are taken under different variations like pose, facial expression, illumination and cluttered background. For GT database, all the face images are cropped and resized to 50×60 pixels to conduct two different experiments. We selected the first eight images of each subject for training and the rest seven images of each subject for testing, to conduct first experiment. In the second experiment, we have used first seven images of each subject for training and the remaining eight images of each subject for testing. The LFW database face images are collected from the web.

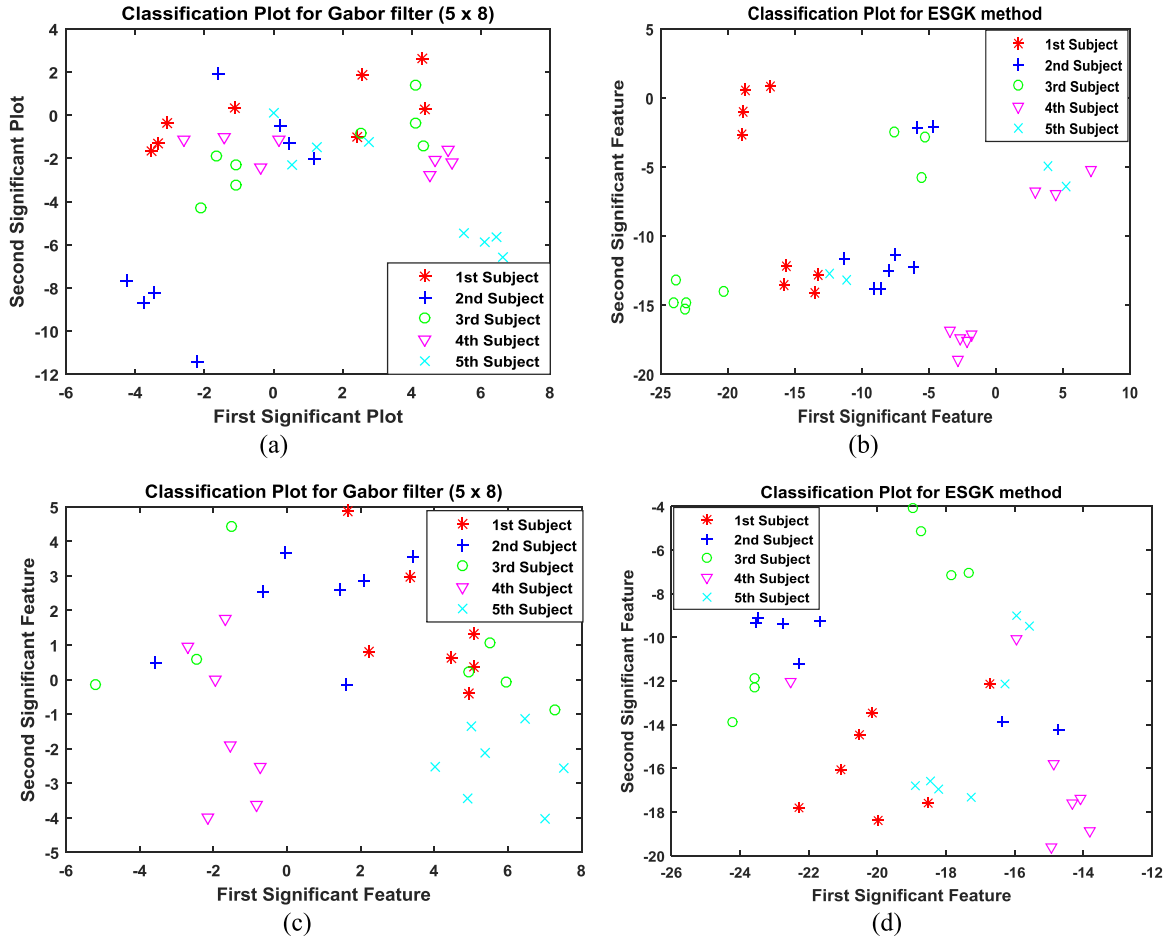

Fig. 14. 2D Classification plots using two most significant features of training face images of LFW database. (a) 40 training images of 5 different subjects obtained using Gabor filter bank (40 filters) method. (b) 40 training images of 5 different subjects obtained using ESGK method. (c) 35 training images of 5 different subjects obtained using Gabor filter bank (40 filters) method. (d) 35 training images of 5 different subjects obtained using ESGK method.

Table 2
Parameters of hybrid PSO-GSA Algorithm.

Parameters	Value
Particle dimension, D	4
Population size, N_S	30
Acceleration co-efficient c_1, c_2	2.0
Acceleration co-efficient c_3, c_4	0.5
Initial value of gravitational constant G_0	100
Constant, α	20
Range of inertia weight (W_{max}–W_{min})	0.9–0.4
Number of iterations	500

From LFW database, we have used a subset of 1251 images of 86 subjects having 11–12 images of each subject. All the face images are manually cropped and resized to 32 × 32 pixels to conduct two different experiments. We have selected the first eight images of each subject for training and the rest images for testing, to conduct the first experiment. In the second experiment, we have used the first seven images of each subject for training and the remaining images for testing. Fig. 9 shows examples of training and test face images from all the five databases.

In this work, the hybrid PSO-GSA is used for optimization after extensive simulation studies. Note that GA, PSO and GSA are also used for optimization. For the purpose of a comparison, the best fitness value obtained from the above optimization techniques are reported in Table 1. From the table, it is observed that hybrid PSO-GSA is able to achieve global minimum as compared to other

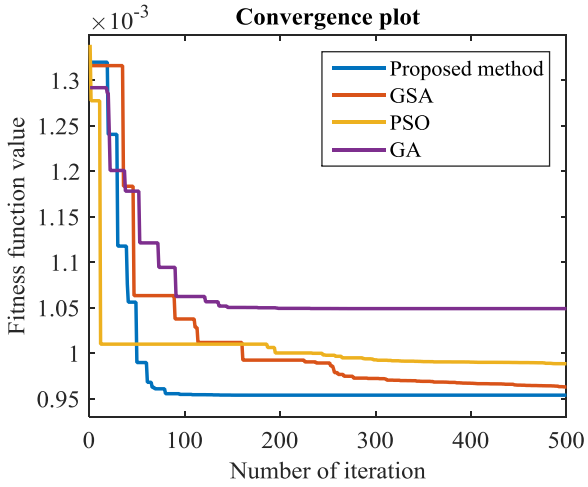

Fig. 15. Convergence plot.

techniques due to its better exploration and exploitation. Further, related experiments to claim the superiority of PSO-GSA over GA, PSO and GSA is also found in Jiang et al. (2014).

Fig. 10 shows the classification plots of face images of the FERET database in 2D space, to demonstrate and compare the class separability measure of Gabor filter bank method with our proposed method. In Fig. 10(a) and (b), 25 face images of 5 different subjects (or classes) are represented in 2D space by taking two most

Table 3
Recognition rate of different methods on FERET database.

Name of the method	Experiment no. 1	Experiment no. 2
PCA+MDC	75.25%	70.17%
LDA+MDC	74.00%	65.83%
Gabor filter bank (3 × 5)+MDC	77.50%	71.50%
Gabor filter bank (5 × 8)+MDC	79.75%	73.83%
Aggregated 2D Gabor Feature-Method+L2-norm	80.00%	75.33%
Proposed method	84.50%	80.50%

Table 4
Recognition rate of different methods on ORL database.

Name of the method	Experiment no. 1	Experiment no. 2
PCA+MDC	91.25%	87.50%
LDA+MDC	90.62%	88.50%
Gabor filter bank (3 × 5)+MDC	88.75%	84.50%
Gabor filter bank (5 × 8)+MDC	92.50%	90.50%
Aggregated 2D Gabor Feature-Method+L2-norm	95.00%	93.50%
Proposed method	97.50%	96.00%

Table 5
Recognition rate of different methods on UMIST database.

Name of the method	Experiment no. 1	Experiment no. 2
PCA+MDC	93.08%	90.94%
LDA+MDC	95.66%	91.97%
Gabor filter bank (3 × 5)+MDC	89.20%	84.98%
Gabor filter bank (5 × 8)+MDC	95.89%	91.74%
Aggregated 2D Gabor Feature -Method+L2-norm	96.36%	92.32%
Proposed method	98.94%	96.33%

Table 6
Recognition rate of different methods on GT database.

Name of the method	Experiment no. 1	Experiment no. 2
PCA+MDC	66.57%	62.25%
LDA+MDC	59.43%	57.50%
Gabor filter bank (3 × 5)+MDC	62.57%	57.75%
Gabor filter bank (5 × 8)+MDC	70.00%	64.25%
Aggregated 2D Gabor Feature-Method+L2-norm	72.86%	68.75%
Proposed method	79.72%	76.25%

Table 7
Recognition rate of different methods on LFW database.

Name of the method	Experiment no. 1	Experiment no. 2
PCA+MDC	15.99%	15.87%
LDA+MDC	10.43%	11.09%
Gabor filter bank (3 × 5)+MDC	10.12%	09.40%
Gabor filter bank (5 × 8)+MDC	16.87%	14.79%
Aggregated 2D Gabor Feature-Method+L2-norm	18.83%	16.95%
Proposed method	39.08%	37.75%

significant features. Similarly, Fig. 10(c) and (d) shows a 2D representation of face images by taking two most significant features from 20 face images of 5 different subjects (or classes). Five symbols are used to represent five different subjects. The plot, in Fig. 10, reveals that features obtained from Gabor filter bank method (Fig. 10(a) and (c)) are not well separated. Some features are even overlapped, resulting in misclassification. However, ESGK method (Fig. 10(b) and (d)) not only separates the different features, but also clusters the same features. This establishes the fact that ESGK method has better class separability measure as compared to the simple Gabor filter method.

Similarly, Figs. 11–14 show the 2D classification plots using two most significant features of training face images of ORL, UMIST, GT and LFW databases, respectively. It is observed that the ESGK method is robust enough to separate features of different face images, besides clustering features of the same subject.

In this paper, we have compared our proposed ESGK method with various existing holistic Gabor bank based FR methods. Boukabou et al. (2006) designed a Gabor filter bank with three scales and five orientations to extract features from training face images. The response of a filter bank having three scales and five orientations to each face images in the training database results in a 24,000-dimension feature vector in FERET database, 15,360-dimension feature vector in ORL database, 15,360-dimension feature vectors in UMIST database, 45,000-dimension feature vector in GT database and 15,360-dimension feature vector in LFW database. These Gabor features are then used to compute statistical features like mean and variance. Euclidean distance measure is used for recognition of unknown test face images. The authors designed the Gabor filter with five scales and eight orientations and used it for FR. Such a filter bank results in a 64,000, 40,960, 40,960, 120,000 and 40,960-dimension feature vectors in FERET, ORL, UMIST, GT and LFW databases, respectively. Aggregated 2D Gabor feature method proposed by Cheung et al. (2004) is also considered in our comparison. In this method, Gabor filter with three scales and eight orientations is used to design a filter bank. Convolution of the training face images with the filter bank is used to obtain features. A filter bank having three scales and eight orientations results in a 38,400, 24,576, 24,576, 72,000 and 24,576-dimension feature vectors in FERET, ORL, UMIST, GT and LFW databases, respectively. Then, low dimensional representation of the Gabor features is obtained by taking their mean and standard deviation. L2-norm is used as the similarity measure for FR.

However, they suffer from high computational cost due to the large dimension feature vectors, obtained from the filter bank. To obtain a Gabor feature vector, each face image is passed through a number of filters in the bank due to which the response time for each face image increases. On the other hand, the proposed ESGK method is capable enough to suppress the problems of high computational cost and large response time. The proposed method includes a single optimized Gabor filter which results in a 1600-dimension feature vector for each face image in FERET database, 1024-dimension feature vector for each face image in ORL database, 1024-dimension feature vector for each face image in UMIST database, 3000-dimension feature vector for each face image in GT database and 1024-dimension feature vector for each face image in LFW database. PCA and LDA methods are also used for a comparison. In PCA and LDA methods, FR is carried out using the minimum distance classifier (MDC). Here, the Euclidean distance is considered.

The hybrid PSO-GSA converges to a global optimum with 500 iterations, to find the optimal Gabor filter parameters. The parameter setting for hybrid PSO-GSA is given in Table 2. In Jiang et al. (2014), it is suggested that the use of parameter values displayed in Table 2 results in a better global optimum convergence as compared to GSA and PSO. Thus, we have also used these parameter values to obtain an optimum Gabor filter. With the given parameter set, PSO-GSA will not show different behaviour to obtain optimum Gabor filter.

The convergence plot of single optimized Gabor filter obtained using different optimization techniques GA, PSO, GSA and hybrid PSO-GSA, is shown in Fig. 15. The plot reveals that the hybrid PSO-GSA converges to a global optimum with 500 iterations, to find the optimal Gabor filter parameters.

The state-of-the-art techniques in connection with a Gabor filter application to FR (within the domain only) have been considered for a comparison. The recognition rate of all the methods on FERET database is listed in Table 3. It is observed that the ESGK method performs better as compared to other methods, with the highest recognition rate of 84.50% and 80.50% in experiment 1 and experiment 2, respectively.

Table 4 shows the recognition rate of all the methods on ORL database. It is observed that ESGK method achieved a high recognition rate of 97.50% and 96.00% in experiment 1 and experiment 2, respectively. Similarly, on the UMIST database ESGK method achieved a high recognition rate of 98.94% and 96.33% in experiment 1 and experiment 2, respectively (Table 5).

The recognition rates of all the methods on the GT and LFW databases are depicted in Tables 6 and 7, respectively. It is observed from Tables 6 and 7, that ESGK gives a high recognition rate as compared to other methods. From all the tables, it is also observed that the recognition rate decreases with a decrease in the number of images in a class (experiment 2). However, ESGK method still performs better as compared to other methods.

From the above tables it is observed that the proposed method yields improved recognition rate. The reason behind this improvement is due to generation of new virtual feature set which includes more face details such as the pose variation, facial expression, occlusion etc. The proposed eigenvalue based classifier represents the test face image as a linear combination of K selected

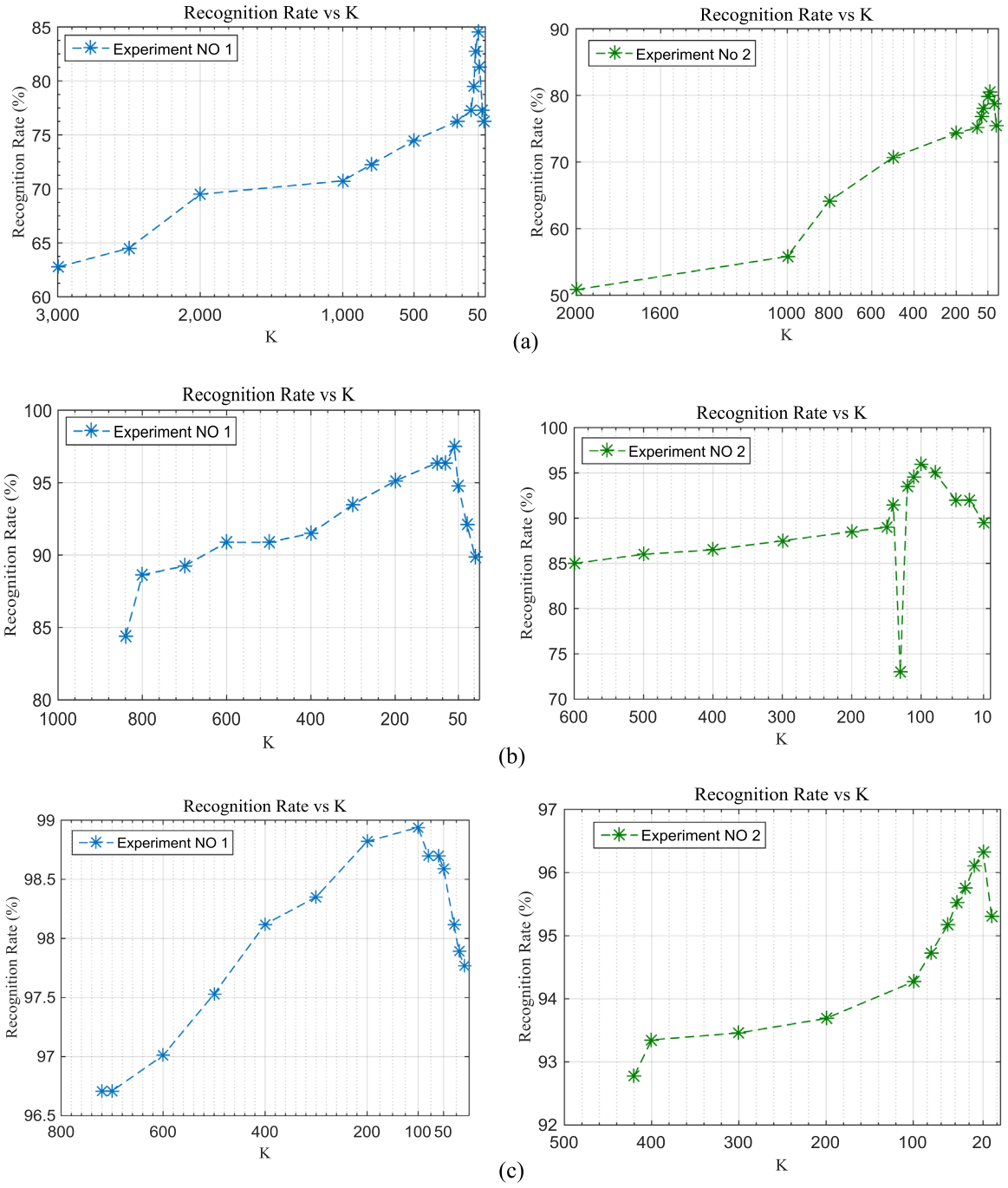

Fig. 16. Variation of recognition rate with K using ESGK method. (a) FERET database. (b) ORL database. (c) UMIST database. (d) GT database. (e) LFW database.

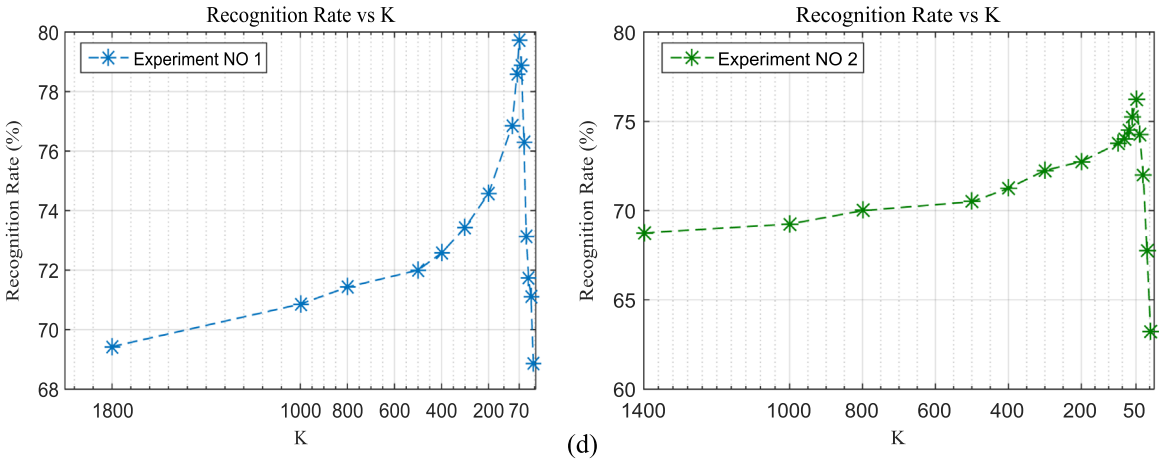

(d)

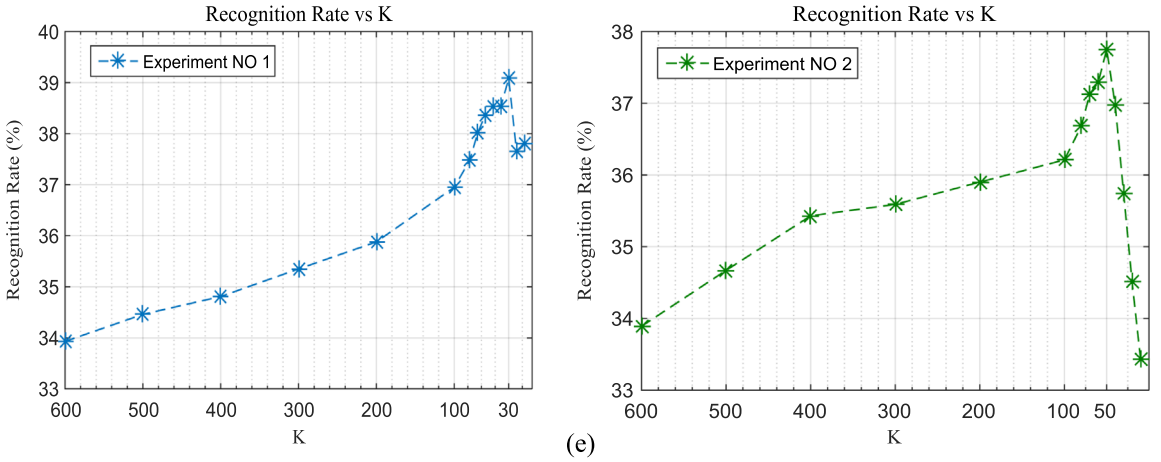

(e)

Fig. 16. (*continued*)

Table 8
Response time of different methods.

Name of the method	Response time in seconds					
	Experiment 1			Experiment 2		
	Gabor filter bank (3×5)	Gabor filter bank (5×8)	Proposed method	Gabor filter bank (3×5)	Gabor filter bank (5×8)	Proposed method
FERET	90.12	234.66	13.86	71.23	187.14	12.74
ORL	20.15	56.37	3.85	15.28	37.67	3.15
UMIST	15.44	36.63	2.42	8.56	21.85	2.53
GT	35.87	92.41	5.24	24.83	65.94	5.03
LFW	62.04	162.00	9.05	42.90	112.02	7.95

useful training images (Eq. (24)). This approach increases the certainty in recognition of test sample even with pose variation and occusion.

Fig. 16 shows the variation of the recognition rate with *K* using the proposed ESGK method on the five databases. On the FERET database, with K =50 a high recognition rate of 84.50% and 80.50% are achieved in the experiment 1 and experiment 2, respectively (as shown in Fig. 16(a)). On the ORL database, in experiment 1, a high recognition rate of 97.50% is recorded with K=50 and in experiment 2 a high recognition rate of 96.00% is recorded with K=100, which is depicted from Fig. 16(b). Here, Fig. 16(c) shows the variation of the recognition rate with K using our proposed method in UMIST database. In experiment 1, a high recognition rate of 98.94% is obtained by K=100 and in experiment 2, 96.33% recognition rate is obtained by K=20. In the GT database, a variation of the recognition rate with K is shown in Fig. 16(d). A high recognition rate of 79.72% is obtained by K=70 in the experiment 1 while 76.25% is obtained by K=50 in the experiment 2. On the LFW database, a high recognition rate of 39.08% and 37.75% is recorded with K=30 and 50 in the experiment 1 and experiment 2, respectively.

We have also compared the response time of our proposed ESGK method with Gabor filter bank method, as shown in Table 8. From the table, it is revealed that our proposed method takes significantly less time for the FR. The reason being use of single filter for feature extraction instead of a filter bank. This idea of implementation of single Gabor filter could be used in many real time applications.

Classification accuracy alone may not provide detailed analysis of a classifier. Therefore, we have used performance measures precision (P), recall (R), F-measure (FM) and similarity metric (SM) to evaluate the robustness of the ESGK method. The performance measures are explained in Wu et al. (2011), Azzopardi and Azzopardi (2013), Huang et al. (2016), Huang et al. (2016, 2014). The value of all these measures lie in the range [0, 1]. A higher value indicates a better classification accuracy.

The result of performance measures of methods in different database using experiment 1 and experiment 2, are presented in Tables 9 and 10, respectively. From Tables 9 and 10, it is observed that the accuracy rates obtained by the proposed ESGK method outperforms all other methods. The reason being the involvement of eigenvalue based classification in the proposed method. The eigenvalue based classification method utilizes only the significant Gabor feature vectors to classify a test face image, by preserving the variance.

Table 9
Performance measures of different methods using Experiment 1.

Database	Measures	Name of the methods					
		PCA	LDA	Gabor bank (3×5)	Gabor bank (5×8)	Aggregated 2D Gabor feature method	ESGK
FERET	P	0.8190	0.8074	0.8476	0.8696	0.8742	**0.9125**
	R	0.8440	0.8320	0.8734	0.8961	0.9006	**0.9403**
	FM	0.8176	0.8060	0.8461	0.8678	0.8734	**0.9109**
	SM	0.7744	0.7635	0.8014	0.8222	0.8271	**0.8628**
ORL	P	0.9357	0.9374	0.9128	0.9432	0.9673	**0.9875**
	R	0.9381	0.9398	0.9151	0.9456	0.9698	**0.9900**
	FM	0.9355	0.9372	0.9126	0.9430	0.9671	**0.9873**
	SM	0.9262	0.9279	0.9036	0.9337	0.9575	**0.9775**
UMIST	P	0.9047	0.9236	0.8668	0.9248	0.9331	**0.9529**
	R	0.9376	0.9571	0.8983	0.9584	0.9670	**0.9875**
	FM	0.9088	0.9278	0.8707	0.9290	0.9373	**0.9572**
	SM	0.8932	0.9118	0.8557	0.9130	0.9214	**0.9407**
GT	P	0.7404	0.6817	0.7071	0.7565	0.7787	**0.8333**
	R	0.7616	0.7012	0.7273	0.7781	0.8009	**0.8571**
	FM	0.7225	0.6652	0.6900	0.7382	0.7598	**0.8131**
	SM	0.6770	0.6233	0.6465	0.6917	0.7120	**0.7619**
LFW	P	0.5858	0.5440	0.5416	0.5939	0.6086	**0.7518**
	R	0.5997	0.5569	0.5545	0.6080	0.6231	**0.7697**
	FM	0.5564	0.5167	0.5145	0.5641	0.5781	**0.7141**
	SM	0.5058	0.4697	0.4677	0.5128	0.5255	**0.6491**

Table 10
Performance measures of different methods using Experiment 2.

Database	Measure	Name of the methods					
		PCA	LDA	Gabor filter bank (3×5)	Gabor filter bank (5×8)	Aggregated 2D Gabor Feature Method	ESGK
FERET	P	0.7919	0.7741	0.7969	0.8064	0.8195	**0.8733**
	R	0.8282	0.8096	0.8335	0.8434	0.8571	**0.9134**
	FM	0.7912	0.7734	0.7963	0.8057	0.8188	**0.8726**
	SM	0.7268	0.7104	0.7314	0.7401	0.7521	**0.8015**
ORL	P	0.9152	0.9198	0.8947	0.9201	0.9501	**0.9700**
	R	0.9177	0.9223	0.8971	0.9226	0.9531	**0.9726**
	FM	0.9144	0.9190	0.8939	0.9192	0.9497	**0.9691**
	SM	0.8987	0.9032	0.8785	0.9035	0.9334	**0.9525**
UMIST	P	0.8842	0.8938	0.8287	0.8935	0.8945	**0.9316**
	R	0.9241	0.9341	0.8661	0.9338	0.9348	**0.9736**
	FM	0.8913	0.9010	0.8354	0.9007	0.9017	**0.9391**
	SM	0.8809	0.8905	0.8256	0.8902	0.8911	**0.9281**
GT	P	0.6982	0.6561	0.6621	0.7134	0.7504	**0.8025**
	R	0.7331	0.6889	0.6952	0.7490	0.7879	**0.8426**
	FM	0.6840	0.6427	0.6486	0.6988	0.7351	**0.7861**
	SM	0.6257	0.5879	0.5933	0.6393	0.6724	**0.7191**
LFW	P	0.5908	0.556	0.5425	0.5828	0.6043	**0.7467**
	R	0.6023	0.5659	0.5531	0.5941	0.6160	**0.7612**
	FM	0.5609	0.5270	0.5150	0.5532	0.5736	**0.7088**
	SM	0.5127	0.4817	0.4707	0.5057	0.5243	**0.6479**

6. Conclusion

In this paper, we have proposed an ESGK method for the FR. Our proposed method has achieved a better performance level as compared to holistic Gabor filter based approaches to FR. The Gabor filter bank is replaced by a single optimal Gabor filter, which significantly reduces both the computational complexity and response time. The hybrid PSO-GSA algorithm is deployed for optimization. However, any other hybrid soft computing technique can be used. The binary-classification-based metrics recall, precision, similarity and F-measure are also computed for a comparison. The proposed eigenvalue based classification method is well suited for the FR. The reason behind the improved recognition rate is due to the generation of virtual feature set using our proposed eigenvalue based classification method. This may lead to the addition of a new dimension in the research area of real time FR. Further, adaptive optimal filters may also be designed for improving the performance.

Acknowledgement

The authors would like to thank the US Army for providing the FERET database for the research work.

References

Abate, A.F., Nappi, M., Riccio, D., Sabatino, G., 2007. 2D and 3D face recognition: a survey. Pattern Recognit. Lett. 28 (14), 1885–1906.
Aradhya, V.M., Pavithra, M.S., 2014. A comprehensive of transforms, Gabor filter and k-means clustering for text detection in images and video. Appl. Comput. Inform. 12, 109–116.
Azzopardi, G., Azzopardi, N., 2013. Trainable COSFIRE filters for keypoint detection and pattern recognition. IEEE Trans. Pattern Anal. Mach. Intell. 35 (2), 490–503.
Barmpoutis, A., Kumar, R., Vemuri, B.C., Banerjee, A., 2008. Beyond the lambertian assumption: a generative model for apparent brdf fields of faces using anti-symmetric tensor splines. Comput. Vision. Pattern Recognit., 1–6.
Blanz, V., Vetter, T., 2003. Face recognition based on fitting a 3D morphable model. IEEE Trans. Pattern Anal. Mach. Intell. 25 (9), 1063–1074.
Boukabou, W.R., Ghouti, L., Bouridane, A., 2006. Face recognition using a Gabor filter bank approach. In: First NASA/ESA Conference on Adaptive Hardware and Systems. pp. 465–468.
Brunelli, R., Poggio, T., 1993. Face recognition: features versus templates. IEEE Trans. Pattern Anal. Mach. Intell. 15 (10), 1042–1052.
Cament, L.A., Galdames, F.J., Bowyer, K.W., Perez, C.A., 2015. Face recognition under pose variation with local Gabor features enhanced by Active Shape and Statistical Models. Pattern Recognit. 48 (11), 3371–3384.
Chellappa, R., Wilson, C.L., Sirohey, S., 1995. Human and machine recognition of faces: a survey. Proc. IEEE 83 (5), 705–741.
Cheung, K.H., You, J., Kong, W.K., Zhang, D., 2004. A study of aggregated 2D Gabor features on appearance-based face recognition. Proc. ICIG, 310–313.
Cruz-Aceves, I., Oloumi, F., Rangayyan, R.M., Aviña-Cervantes, J.G., Hernandez-Aguirre, A., 2016. Automatic segmentation of coronary arteries using Gabor filters and thresholding based on multiobjective optimization. Biomed. Signal Process. Control. 25, 76–85.
Daugman, J.G., 1985. Uncertainty relation for resolution in space, spatial frequency, and orientation optimized by two-dimensional visual cortical filters. JOSA A 2 (7), 1160–1169.
Daugman, J.G., 1988. Complete discrete 2-D Gabor transforms by neural networks for image analysis and compression. IEEE Trans. Acoust. Speech Signal Process. 36 (7), 1169–1179.
Huang, S.C., Jiau, M.K., Hsu, C.A., 2014. A high-efficiency and high-accuracy fully automatic collaborative face annotation system for distributed online social networks. IEEE Trans. Circuits Syst. Video Technol. 24 (10), 1800–1813.

Huang, S.C., Jiau, M.K., Jian, Y.H., 2016. Optimisation of automatic face annotation system used within a collaborative framework for online social networks. IET Comput. Vision. 10 (5), 349–358.
Huang, Y., Guan, Y., 2015. On the linear discriminant analysis for large number of classes. Eng. Appl. Artif. Intell. 43, 15–26.
Jiang, S., Ji, Z., Shen, Y., 2014. A novel hybrid particle swarm optimization and gravitational search algorithm for solving economic emission load dispatch problems with various practical constraints. Int. J. Electr. Power Energy Syst. 55, 628–644.
Jones, J.P., Palmer, L.A., 1987. An evaluation of the two-dimensional Gabor filter model of simple receptive fields in cat striate cortex. J. Neurophysiol. 58 (6), 1233–1258.
Kennedy, J., Eberhart, R.C., 1995. Particle swarm optimization. In: Proceedings of the IEEE International Conference on Neural Networks, Piscataway, pp. 1942–1948.
Kruizinga, P., Petkov, N., 1999. Nonlinear operator for oriented texture. IEEE Trans. Image Process. 8 (10), 1395–1407.
Lades, M., Vorbruggen, J.C., Buhmann, J., Lange, J., von der Malsburg, C., Wurtz, R.P., Konen, W., 1993. Distortion invariant object recognition in the dynamic link architecture. IEEE Trans. Comput. 42 (3), 300–311.
Li, A., Shan, S., Gao, W., 2012. Coupled bias–variance tradeoff for cross-pose face recognition. IEEE Trans. Image Process. 21 (1), 305–315.
Li, L., Jin, L., Xu, X., Song, E., 2013. Unsupervised color–texture segmentation based on multiscale quaternion Gabor filters and splitting strategy. Signal Process. 93 (9), 2559–2572.
Li, X., Mori, G., Zhang, H., 2006. Expression-invariant face recognition with expression classification. In: Proceedings of the 3rd Canadian Conference on Computer and Robot Vision (CRV'06), pp. 77–77.
Liu, C., Wechsler, H., 2003. Independent component analysis of Gabor features for face recognition. IEEE Trans. Neural Netw. 14 (4), 919–928.
Manikandan, S., Ramar, K., Iruthayarajan, M.W., Srinivasagan, K.G., 2014. Multilevel thresholding for segmentation of medical brain images using real coded genetic algorithm. Measurement 47, 558–568.
Matthew, T.U.R.K., 2001. A random walk through eigenspace. IEICE Trans. Inf. Syst. 84 (12), 1586–1595.
Paysan, P., Knothe, R., Amberg, B., Romdhani, S., Vetter, T., 2009. A 3D face model for pose and illumination invariant face recognition. Adv. Video Signal Based Surveill., 296–301.
Perez, C.A., Cament, L.A., Castillo, L.E., 2011a. Local matching Gabor entropy weighted face recognition. Autom. Face Gesture Recognit. Workshops, 179–184.
Perez, C.A., Cament, L.A., Castillo, L.E., 2011b. Methodological improvement on local Gabor face recognition based on feature selection and enhanced Borda count. Pattern Recognit. 44 (4), 951–963.
Phillips, P.J., Moon, H., Rizvi, S.A., Rauss, P.J., 2000. The FERET evaluation methodology for face-recognition algorithms. IEEE Trans. Pattern Anal. Mach. Intell. 22 (10), 1090–1104.
Phillips, P.J., 2004. The facial recognition technology (FERET) database. Online: ⟨http://www.itl.nist.gov/iad/humanid/feret/feret_master.html⟩.
Raghavendra, U., Acharya, U.R., Fujita, H., Gudigar, A., Tan, J.H., Chokkadi, S., 2016. Application of Gabor wavelet and Locality Sensitive Discriminant Analysis for automated identification of breast cancer using digitized mammogram images. Appl. Soft Comput. 46, 151–161.
Rashedi, E., Nezamabadi-Pour, H., Saryazdi, S., 2009. GSA: a gravitational search algorithm. Inf. Sci. 179 (13), 2232–2248.
Serrano, Á., de Diego, I.M., Conde, C., Cabello, E., 2011. Analysis of variance of Gabor filter banks parameters for optimal face recognition. Pattern Recognit. Lett. 32 (15), 1998–2008.
Shah, J.H., Sharif, M., Raza, M., Azeem, A., 2013. A survey: linear and nonlinear PCA based face recognition techniques. Int. Arab J. Inf. Technol. 10 (6), 536–545.
Shen, L., Bai, L., 2006. A review on Gabor wavelets for face recognition. Pattern Anal. Appl. 9 (2–3), 273–292.
Sun, Z., Bebis, G., Miller, R., 2005. On-road vehicle detection using evolutionary Gabor filter optimization. IEEE Trans. Intell. Transp. Syst. 6 (2), 125–137.
Vu, N.S., Caplier, A., 2009. Efficient statistical face recognition across pose using local binary patterns and Gabor wavelets. Biom.: Theory Appl. Syst., 1–5.
Wang, S.J., Yang, J., Sun, M.F., Peng, X.J., Sun, M.M., Zhou, C.G., 2012. Sparse tensor discriminant color space for face verification. IEEE Trans. Neural Netw. Learn. Syst. 23 (6), 876–888.
Wiskott, L., Fellous, J.M., Kuiger, N., Von Der Malsburg, C., 1997. Face recognition by elastic bunch graph matching. IEEE Trans. Pattern Anal. Mach. Intell. 19 (7), 775–779.
Wu, Z., Ke, Q., Sun, J., Shum, H.Y., 2011. Scalable face image retrieval with identity-based quantization and multireference reranking. IEEE Trans. Pattern Anal. Mach. Intell. 33 (10), 1991–2001.
Xu, Y., Fang, X., Li, X., Yang, J., You, J., Liu, H., Teng, S., 2014. Data uncertainty in face recognition. IEEE Trans. Cybern. 44 (10), 1950–1961.
Zhao, Z.S., Zhang, L., Zhao, M., Hou, Z.G., Zhang, C.S., 2012. Gabor face recognition by multi-channel classifier fusion of supervised kernel manifold learning. Neurocomputing 97, 398–404.
Zou, J., Ji, Q., Nagy, G., 2007. A comparative study of local matching approach for face recognition. IEEE Trans. Image Process. 16 (10), 2617–2628.